2022

Modeling of an Ultra-Low Temperature Refrigeration System for Independent Vaccines and Medical Supplies Storage

Abd Alrhman Mohammad Bani Issa

Elias N. Pergantis

John K. Brehm

Eckhard A. Groll

Davide Ziviani

Modeling of an Ultra-Low Temperature Refrigeration System for Independent Vaccines and Medical Supplies Storage

Abd Alrhman M. BANI ISSA[1]*, Elias N. PERGANTIS[1], John K. BREHM[1], Eckhard A. GROLL[1], Davide ZIVIANI[1]

[1]Ray W. Herrick Laboratories, School of Mechanical Engineering, Purdue University, West Lafayette, IN, USA
abaniiss@purdue.edu; epergantis@purdue.edu; brehm3@purdue.edu; groll@purdue.edu; dziviani@purdue.edu

* Corresponding Author

ABSTRACT

The need for low-temperature refrigeration systems to maintain and transport vaccines and other medical supplies has grown since the emergence of the COVID-19 pandemic. Current technologies are characterized by capacity limitations and inefficient performance. Therefore, there is a need to design new systems that overcome these difficulties. Although low-temperature refrigeration systems still benefit from HFC replacement exceptions, the ongoing phase-down of existing HFC refrigerants requires additional research to identify low global warming potential (GWP) substitutes. Some COVID-19 vaccines must be stored at ultra-low temperatures (ULT) between -90 °C and -60 °C to prevent doses spoilage. Other medical supplies, for example, antibiotics and plasma, require storage temperatures of roughly -20 °C. Therefore, multi-temperature refrigerated containers are typically used to deliver medical supplies globally. This study investigates different low-GWP refrigerants and cycle architectures for a two-compartment refrigeration system. As such, the cascade cycle architecture has been found to provide the highest coefficient of performance (COP) compared to other vapor compression cycles. This work examines five multi-stage compressor cascade cycles, each with its economizer configuration, with the refrigerants selected to be propane (R290) and ethane (R170) for the high and low-stage cycles, respectively. The proposed systems were compared under the same operating conditions to a simple cascade cycle with R404A/R508B as the refrigerant pair, representing the most used architecture for ULT refrigeration systems. Both first and second laws of thermodynamics were employed to quantify cycle and component irreversibilities along with opportunities for further optimizations. Finally, design recommendations at different boundary and operating conditions are presented.

1. INTRODUCTION

The sudden emergence of COVID-19 has put the world in a serious situation, causing the death of roughly six million people and resulting in over 400 million confirmed cases (WHO, 2022). Fortunately, the international community quickly remedied the situation by rapidly adopting anti-disease actions. Among these measures are vaccine discovery, manufacturing, and distribution. The high demand for vaccination increased the need for low-temperature refrigeration systems to maintain and deliver them safely. For instance, Pfizer vaccine must be kept between -90°C and -60°C to prevent the doses from spoiling; Moderna's COVID-19 vaccine requires temperatures of between -25°C and -15°C to be preserved, while Janssen vaccine is typically stored at a temperature ranging between 2°C and 8°C (CDC, 2021). Not only do different vaccines require unique storage temperatures but also every vaccine needs various temperatures in the different stages of their handling and transportation. Special attention should be given to the design process of refrigeration systems to account for all these variables.

According to the American Society of Heating, Refrigerating and Air-Conditioning Engineers (ASHRAE), refrigeration systems that operate at temperatures below -50°C are referred to as ultra-low temperature (ULT) systems (ASHRAE, 2018). ULT refrigeration systems can be found in vaccine warehouses and transport containers. A typical cold chain logistics for an effective distribution of vaccines is presented in Hwang *et al.* (2022) and Mouneer *et al.* (2021). The International Air Transport Association (IATA) estimates that 20% of the temperature-sensitive vaccine shipments get deteriorated during transportation (Chawla, 2020).

Two technologies have been commonly used for ULT transportation systems, namely thermal shipping containers and ultra-cold refrigerators. Generally, both methods provide a temperature in the range between -60 °C and -90 °C. The

thermal shipping container is a passive (non-electrical) method that uses dry ice (solid form of carbon dioxide) in insulated boxes to maintain the needed temperatures. This approach is characterized by limited temperature control, short storage time (~30 days), restrictions on the number and period of the container opening, and the risk of asphyxiation. Consequently, the thermal shipping container is considered as a temporary storage alternative. ULT refrigerators, on the contrary, are purpose-built electrically driven devices that use the vapor-compression refrigeration cycle (or other refrigeration cycles) as their working principle. They can store vaccines until their expiration date, making them by far the most reliable option (CDC, 2021) (Pfizer, 2022).

Single-refrigerant cycles are not recommended for this application for multiple of reasons. High discharge temperatures and compression ratios are two limiting factors. Even if we overcome these difficulties with a multi-compression system, the lack of a single refrigerant that operates in this large temperature range makes this option impractical. Therefore, the typical cycle architecture for ULT refrigerators is the two-stage cascade cycle (Stegmann, 2000). Two or more vapor-compression cycles with different refrigerants are employed in the cascade refrigeration system. The two circuits are coupled by a heat exchanger that acts as a condenser for the low-stage refrigerant and evaporator for the high-stage one. Typically, R22, R507, or R404A are employed in the high-temperature circuit, while R23 or R508B are in the low-temperature circuit (ASHRAE, 2018). Although the cascade cycle is considered successful for ULT refrigeration applications, it suffers from inefficient performance and frost formation.

Liu *et al.* (2012) experimentally investigated the feasibility of a dual-mode cascade refrigeration cycle (low-temperature cycle alone or with the high-temperature cycle). Boahen and Choi (2017) reviewed the recent works conducted on cascade heat pumps for heating and refrigeration applications. They mentioned the need for additional research on refrigerant charge amount, cascade heat exchanger types, and control strategies for matching part-load capacities with variable speed compressors. Eini *et al.* (2016) performed a multi-objective optimization that considers exergetic, economic, environmental, and the inherent safety level of a cascade refrigeration system.

Another less common architecture used for ULT refrigeration is the auto-cascade. This system utilizes a mixture of two refrigerants with different thermophysical and saturation properties as the working fluid such as one operating on the evaporator side and the mixture on the condenser side. The refrigerants are mixed and compressed through a single compressor. To minimize thermodynamic losses in the throttling process, the auto-cascade cycle can be modified by incorporating an ejector (Babiloni *et al.*, 2020). Aprea and Maiorino (2009) achieved a temperature of −150°C with an auto-cascade refrigeration system. Compared to conventional cascades, the auto-cascade requires only one compressor and is better in lubricant oil return but endures reductions in energy efficiency as well as frost accumulation (Hwang *et al.*, 2022). The system is also complicated in terms of its chemistry and refrigerant compositions. A thermodynamic analysis of auto-cascade refrigeration cycles, with and without ejector, for ULT applications using a mixture of R600a/R1150 is introduced in Rodríguez-Jara *et al.* (2022). Recently, the reverse Brayton cycle, with air as the working fluid, was suggested to overcome the difficulties found in other conventional technologies (Brehm *et al.*, 2022).

Refrigerant selection is an important task for any refrigeration system. In addition to the absence of refrigerants that works in the desired temperature range, the refrigerants should honor (1) the Montreal protocol promoting the use of refrigerants with zero ozone depletion potential (ODP); and (2) the Kigali protocol pushing for the use of refrigerants which have a low global warming potential (GWP). Although for the time being, laws banning high GWP refrigerants have excluded ULT applications such as Regulation (EU) No 517/2014 (European Laws Database, 2014), this is expected to change with its market share having increased rapidly in the last two years. As described in many national (DOE E3 Initiative) and international (IPCC AR6, IEA Heat Pumps 2018) reports and initiatives, there is a drive to discover novel low GWP and high-performance refrigerants. Babiloni *et al.* (2020) examined several options of refrigerant pairs for ULT cascade systems and recommended the use of R170 and R1150 for the low-temperature cycle if their flammability is not a concern or otherwise R1132a is preferable.

Multi-stage compression with economization is often employed in heating and refrigeration systems when a large discharge temperature and pressure difference is required between the evaporator and condenser. Economization can be either open, when saturated vapor and liquid are separated in a flash tank, or closed, where upstream extraction through an expansion valve is used. The intermediate compression pressure can be controlled to maximize the cycle's COP. With the rise in demand for cold-climate heating and ULT refrigeration systems using natural refrigerants, multi-stage compression with economization has gained academic traction. Work has focused on low-GWP drop-in replacements of current refrigerants (Sun *et al.*, 2020), transcritical CO_2 cycles (Sarkar and Agrawal, 2010), and cold climate heat pumps (Bertsch and Groll, 2008). This work is novel in applying economization to cascade cycles for ultra-low temperature applications and investigating the impact of different forms of economization.

To this end, this paper aims to design a two-evaporator refrigeration cycle for a two-compartment shipping or storage container with the following specifications:

1. Two-compartment system with two distinct temperatures, one of them is devoted to ULT applications.

2. The use of environmentally friendly refrigerants.
3. Higher performance compared to conventional systems.

2. SYSTEM DEFINITION

This paper aims to analyze a two-temperature refrigeration system for a two-compartment shipping or storage container. The temperature of one compartment should be kept at -20 ℃ (compartment 1), while the other at -70 ℃ (compartment 2). The desired total cooling capacity is 2 tons of refrigeration, with a third of the load needed to cool compartment 1 and the rest for compartment 2. The system will be designed to operate at an outdoor temperature ranging between -10℃, representing the northeastern United States in winter, and 50 ℃ for a summer day in Sub-Saharan Africa. The container will be accessible through one door only so that the MT section can be used as an airlock to avoid energy losses. Arpagaus *et al.* (2016) summarized several multi-temperature heat pump cycle configurations, highlighting their advantages and challenges. They revealed that multi-stage compression with economization and cascade cycles have the highest COPs and second law efficiencies among other multi-temperature cycle architectures. Since the cascade cycle is convenient for ULT applications, it will be selected for further analysis and development.

Optimization of the system's performance requires the selection of the appropriate refrigerant pair along with suitable cycle architecture. One way to improve the cycle performance without excessively increasing its complexity is by adding a second-stage compression with economization to one of the circuits. Several cycle configuration options arise with this modification, depending on the type of economization (open or closed economization), the cycle to be adjusted (high or low-stage cycle), and the location of the MT evaporator. The first and second laws of thermodynamics will be used under the same operating conditions to assess if one of these systems performs better than the others. Figure 1 demonstrates the schematics of the selected cycles for analysis.

A simple cascade cycle (Base cycle) with R404A/R508B refrigerant pair for the high and low-stage cycles, as shown in Figure 1 (a), is used as a reference for comparison with other cycles. The MT evaporator is connected in series with the cascade heat exchanger (HX) in the high-stage cycle as indicated in Arpagaus *et al.* (2016). Selected cycles for analysis are numbered from 1 to 5 and described in Table 1. Each cycle consists of three compressors, five heat exchangers (two evaporators, one condenser, cascade HX, economizer) with exception of Cycle 1 where the economizer is replaced with a flash tank, three expansion valves, and accessories.

One evaporator is dedicated to each compartment, and the condenser is exposed to the outdoor ambient temperature. The economizer benefits the system by increasing the enthalpy difference across the evaporator while reducing the compressor's discharge temperature, which is expected to be high with high-pressure ratios. A closed economizer with upstream extraction was selected for four systems as our choice for the economizer because of its ability to accurately control the suction state of the upper stage compressor. Only Cycle 1 uses a flash tank to evaluate the performance deterioration when using closed economization; closed economization should be preferable if the difference in efficiency is small. It is also possible to run the system with a single-stage compression, i.e., bypass the lower compressor, with additional piping. This is extremely useful at low outdoor temperatures when the gain with two-stage compression cannot be justified economically. The expansion valves' opening is adjusted automatically to maintain a constant superheat at the compressors' suction states.

The systems, however, may encounter some issues in optimizing the injection-line mass flow rate. Therefore, a tradeoff between higher system performance and higher evaporator mass flow rate should be considered. Furthermore, an oil management system may need to be integrated with the systems to allow for safe operation.

Table 1: Description of the selected cycles

Configuration	Economization Type	Cycle with Economization	MT Evaporator Location
Cycle 1	Flash Tank	High-Stage	In series with the cascade HX
Cycle 2	Closed Economizer	High-Stage	In series with the cascade HX
Cycle 3	Closed Economizer	High-Stage	Injection line
Cycle 4	Closed Economizer	Low-Stage	Injection line
Cycle 5	Closed Economizer	Low-Stage	In series with the cascade HX

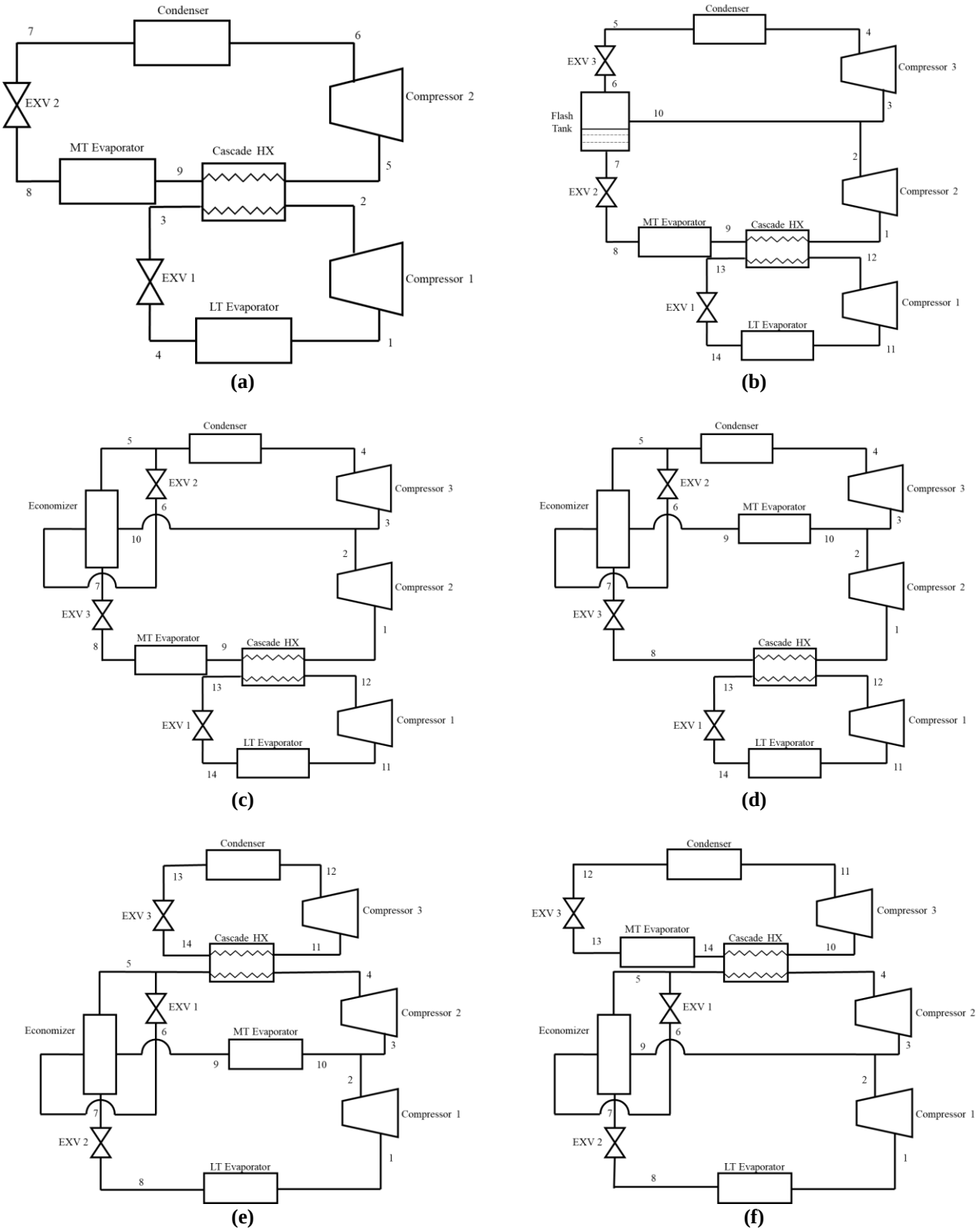

Figure 1: Schematic diagrams of the selected multi-temperature refrigeration cycles for ULT applications: (a) Base Cycle, (b) Cycle 1, (c) Cycle 2, (d) Cycle 3, (e) Cycle 4, and (f) Cycle 5

3. THERMODYNAMIC MODELING

A thermodynamic model was developed to investigate the performance of the cycles compared to the base cycle and a reference equivalent Carnot cycle in the case of multi-source temperatures. The calculations are based on the steady-state first and second laws of thermodynamics and the mass balance equations, which are described mathematically below.

$$\sum_{in} \dot{m} - \sum_{out} \dot{m} = 0 \tag{1}$$

$$\dot{Q} - \dot{W} + \sum_{in} \dot{m}\left(h + \frac{V^2}{2} + gz\right) - \sum_{out} \dot{m}\left(h + \frac{V^2}{2} + gz\right) = 0 \tag{2}$$

$$\sum_{i} \frac{\dot{Q}_i}{T_{b,i}} + \sum_{in} \dot{m}s - \sum_{out} \dot{m}s \; + \dot{S}_{gen} = 0 \tag{3}$$

$$\dot{E}x_{dest} = T_{amb}\dot{S}_{gen} \tag{4}$$

The following assumptions were utilized in the cycle models:

1. Steady-state steady-flow analysis.
2. Kinetic and potential energy effects of fluid streams entering and exiting any control volume are negligible.
3. Negligible pressure drops and heat losses to the surrounding in heat exchangers and piping.
4. Adiabatic compressors with isentropic efficiency according to Bahman *et al.* (2022).

$$\eta_{is} = 0.85 - 0.046667\frac{P_2}{P_1} \tag{5}$$

5. Adiabatic expansion valves with isenthalpic expansion.
6. The refrigerant leaves the evaporators with superheating $\Delta T_{SH} = 5$ ℃ and the condensers with subcooling $\Delta T_{SC} = 5$ ℃ with reference to the evaporation and condensation temperatures, respectively.
7. The evaporation and condensation temperatures of the refrigerant were selected with a 10 ℃ difference from the heat sources and sink.
8. The cascade heat exchangers were modeled with a 5 °C difference between the condensation temperature of the low-stage cycle and the evaporation temperature of the high-stage cycle.
9. The economizers were designed such that the temperature difference across it is equal to 10 ℃.
10. The pressure at the injection line is assumed to be the geometric mean of the evaporation and condensation pressures, as recommended by Stoecker (1998).

The details of the model across each component are not mentioned because of space limitations. The cascade pressure in Cycles 3 and 4 was optimized using the Golden-section search technique such that it maximizes the cycles' COP. The Engineering Equation Solver (EES) (Klein and Alvarado, 2002) was used to solve the set of equations and to evaluate the properties of the working fluids.

Two performance indices were used to quantify the comparison between cycles. First, the coefficient of performance (COP), which is defined as the ratio of the cooling capacity to the total power requirement to run the cycle. Mathematically, the COP can be described as:

$$\mathrm{COP} = \frac{\dot{Q}_{evap,LT} + \dot{Q}_{evap,MT}}{\sum_i \dot{W}_{comp,i}} \tag{7}$$

The other parameter used for cycle evaluation is the second law efficiency (ϵ). It is defined as the ratio of the actual cycle COP to the Carnot COP (COP_C) and accounts for the cycle irreversibilities. Generally, the Carnot COP is found as the absolute heat source temperature divided by the ambient and source temperature difference. However, a new definition is needed with two evaporation temperatures. Arpagaus *et al.* (2016) proposed using a weighted average

factor β of the two heat sources to solve the problem. The equivalent Carnot COP can then be found as per equations 8-10.

$$\beta = \frac{\dot{Q}_{evap,MT}}{\dot{Q}_{evap,MT} + \dot{Q}_{evap,LT}} \tag{8}$$

$$\alpha = \frac{\beta}{1-\beta}\frac{COP_{C,LT}}{COP_{C,MT}} \tag{9}$$

$$\mathrm{COP_C} = \frac{1}{1+\alpha}\mathrm{COP_{C,LT}} + \frac{\alpha}{1+\alpha}\mathrm{COP_{C,MT}} \tag{10}$$

4. RESULTS AND DISCUSSION

The simulation results will be summarized in the following two sections. Section 4.1 considers various alternatives of working fluids pairs and evaluates them based on several criteria, while Section 4.2 compares the performance of the cycle configurations described in Section 2.

4.1 Working Fluids Selection

The refrigerants presented in Table 2 have been selected based on the requirement that the temperature range of each circuit (MT or LT) is between their normal boiling point and critical temperature. High GWP refrigerants have also been included. It was found that the refrigerants of which the performance was highest (~5-10% COP increase from mean value) also had a low $GWP_{100yr} < 20$, the exception being R41 (Methyl Fluoride) and R32 (Difluoromethane). Although some refrigerants had comparable performance to those of their natural counterparts, those being R143a, R22, R410A, and R507A (HFCs) on the MT side and R13 (CFC, banned), R23, and R508B (HFCs) on the LT side, their low flammability (A1) and decent performance are outweighed by their high GWP and the gradual down-phasing of HFCs. It should be noted that the industry standard is using R507A on the MT loop and either R32 or R508B on the LT temperature one.

Both ethane (R170) and ethylene (R1150) are recommended for the LT cycle, although ethylene is the better choice for $T_{LT} < -90$°C. Our findings are along the lines with Sun *et al.* (2019) and *Sarkar et al.* (2013) on which refrigerants offer the best performance in a cascade system; however, these authors' work has only been focused on single compartment system. R170 refrigerant demonstrates higher isentropic and volumetric efficiencies as well as a lower pressure ratio over other refrigerants (Abas *et al.*, 2018). To identify which refrigerant combination offers the best COP against various ambient conditions, the eight most promising combinations have been presented in Figure 2.

Based on the results in Figure 2, it is shown that R290/R170 is the best performing MT/LT pair, with a 10.2% COP increase over the second-best performing pair, R161/R170, and 58.7% over the worst performing, R1234yf/R41. The performance enhancement of using R290/R170 is even more prominent at high ambient temperatures. This agrees with Sun et al. (2019) and disagrees with Mohammadi and Powel (2021), who did not account for varying compressor efficiencies. The second-best performing pair is R161/R170. However, R290 should be preferred given that R161 has only gained traction in the last ten years and because R290 has a higher COP with identical GWP. Investigating the flammability risk of using R290/R170 requires detailed component sizing, which involves analyzing potential leakages from the system. Preventative measures, such as packaging the system and limiting its use for external applications, would also reduce flammability risks.

4.2 Cycles Comparison

The thermodynamic model was executed for an outdoor temperature ranging from -10°C to 50°C for the proposed systems in Section 2. The results were compared under the same operating conditions to the base cycle with R404A/R508B (Base 1) and R290/R170 (Base 2) as working fluid pairs. Cycles 1, 2, and 4 showed the same performance over the entire temperature range. Similarly, Cycles 3 and 5 did. The reason for this is that they will have the same compression ratio under optimized conditions.

Figure 3 illustrates the COP and second law efficiency for Cycle 2, Cycle 3, and the base cycle. Other cycles were overlooked for sake of figure clarity since they can be represented precisely with the given cycles. Cycle 2 provides an average gain of 80.33% in COP compared to Base 1 and 37.85% to Base 2 over the entire temperature range. The enhancement increases with the outdoor temperature despite the overall decrease in performance with temperature. Cycle 2 is recommended for high outdoor temperature applications with the highest efficiency ($\epsilon = 31.19\%$) at a

temperature equal to 24°C. On the other hand, Cycle 4 shows contradictory behavior, with most improvements occurring at low temperatures and decaying with ambient temperatures. The average COP enhancement is 58.11% and 25.80% compared to Base 1 and Base 2, respectively. Clearly, there is no preference for one system over the other at a temperature of 21°C, and all systems perform similarly.

Table 2: Refrigerant Properties and Performance in Base Cycle

	Refrigerant	NBP/ °C	Critical Temperature/ °C	ODP	GWP_{100yr}	Safety Classification	COP†, ‡
HTC	**R290**	**-42.1**	**96.7**	**0**	**~10**	**A3**	**0.71**
	R717	-33.3	132.4	0	<1	B2L	0.56
	R115	-39.2	79.9	0.4	7370	A1	0.64
	R12	-29.7	112.0	1	10900	A1	0.68
	R1216	-30.3	85.7	0	<1	B3	0.59
	R1234yf	**-29.5**	**94.7**	**0**	**4**	**A2**	**0.63**
	R125	-48.1	66	0	3500	A1	0.64
	R134a	-26.1	101.1	0	1430	A1	0.59
	R143a	-47.2	72.7	0	4470	A2	0.68
	R161	**-37.5**	**102.1**	**0**	**12**	**A3**	**0.68**
	R218	-36.8	71.9	0	8830	A1	0.55
	R22	-40.8	96.1	0.05	1810	A2L	0.68
	R32	**-51.6**	**78.1**	**0**	**675**	**A2L**	**0.68**
	R404A	-46.2	72.1	0	3900	A1	0.65
	R407C	-43.6	86.2	0	1774	A1	0.51
	R410A	-51.4	71.3	0	2088	A1	0.67
	R507A	-46.7	70.6	0	3985	A1	0.66
LTC	**R170**	**-78.5**	**32.1**	**0**	**~10**	**A3**	**0.71**
	R1150	-103.7	9.2	0	~10	A3	0.70
	R116	-78	19.9	0	12200	A1	0.6
	R13	-81.5	28.9	1	14400	A1	0.65
	R23	-82	26.1	0	14800	A1	0.59
	R508B	-88	12.1	0	13,396	A1	0.65
	R41	**-78.3**	**44.1**	**0**	**97**	**A2**	**0.59**

† COP on the HTC was obtained using T_{amb} = 21°C and R170 as the LT refrigerant.
‡ COP on the LTC was obtained using T_{amb} = 21°C and R290 as the HT refrigerant.

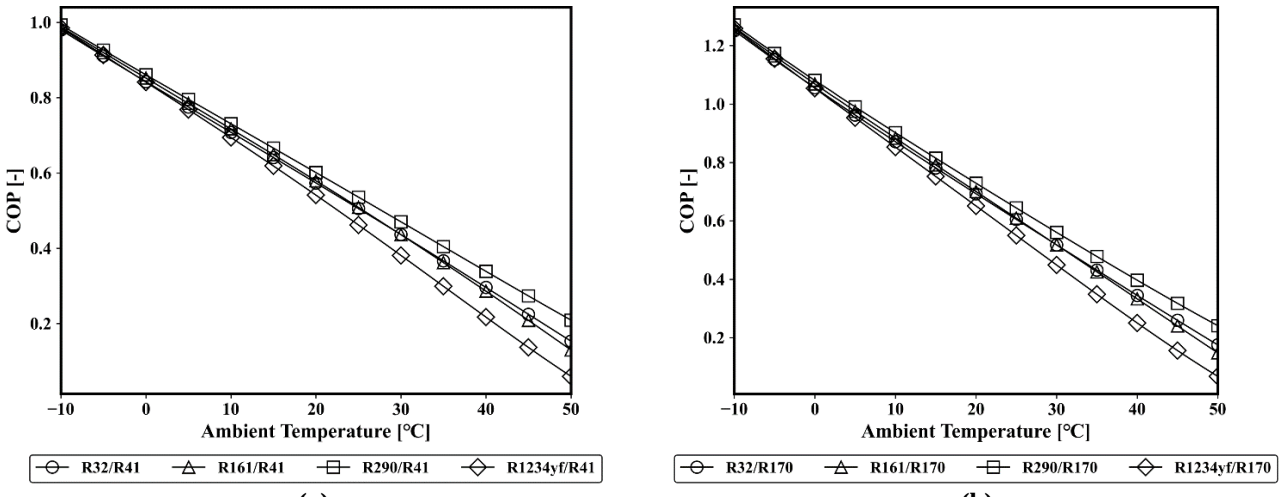

Figure 2: Performance of different HT refrigerants in the base system for (a) LT refrigerant being R41 and (b)LT refrigerant being R170

The required power for running Cycle 2 was 6.79 kW, with irreversibilities contributing 68.8% of this value (4.68 kW). Compressor 1 and the cascade HX have the highest share of irreversibilities. Each component's irreversibility contribution for Cycle 2 is shown in Figure 4 (a). Similar power consumption and irreversibility values are expected in Cycle 3, but with Compressor 3 and the condenser causing the most of irreversibility, as presented in Figure 4 (b).

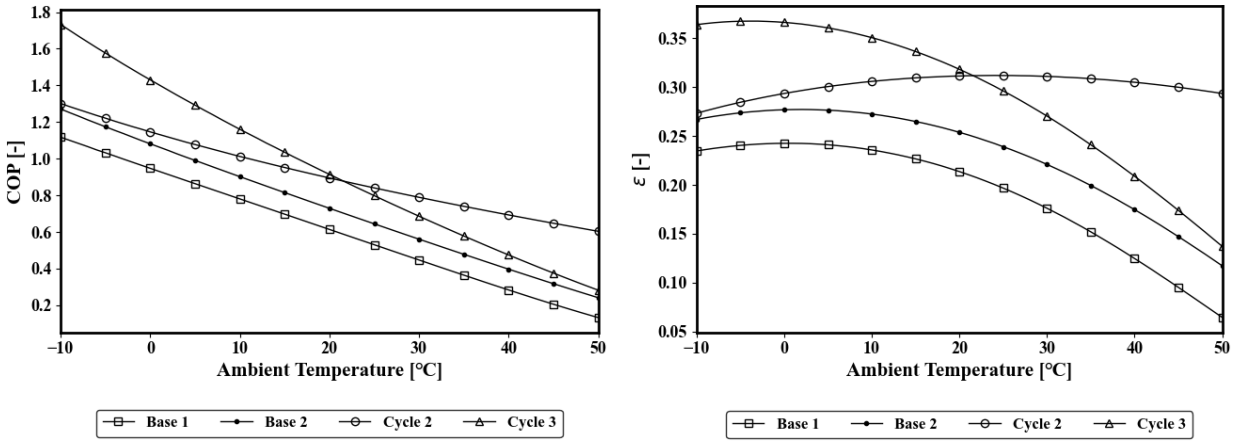

(a) **(b)**

Figure 3: Performance of different cycle configurations over ambient temperature (a) COP and (b) Second law efficiency

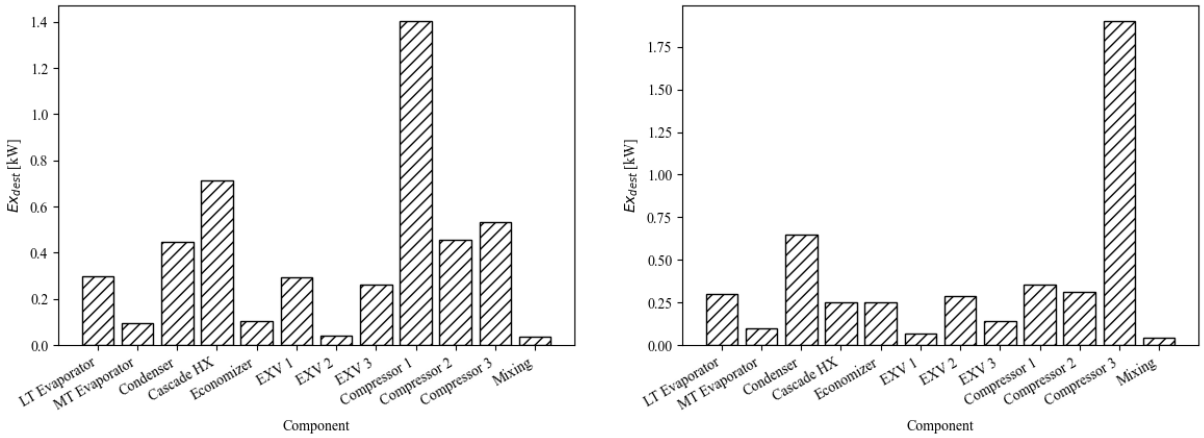

(a) **(b)**

Figure 4: Exergy destruction for each cycle component (a) Cycle 2 and (b) Cycle 3

To take advantage of the distinguished performance characteristics of Cycle 3 at low ambient temperatures and Cycle 2 at high temperatures, a novel system is proposed to operate at dual modes based on the outdoor temperatures, as shown in Figure 5. The new architecture requires the MT evaporator to be connected to an eight-way valve, so it operates on the injection line (similar to Cycle 3) or next to the cascade heat exchanger (similar to Cycle 2) depending on outdoor conditions. We can achieve an average improvement of 92.3% compared to Base 1 and 48.3% relative to Base 2 over the entire temperature range. However, additional control of the system is necessary.

5. CONCLUSIONS

A multi-stage compression cascade cycle with closed economization architecture using the natural pair (R290/ R170) as refrigerants has been proposed for ULT refrigeration applications. A target cooling capacity of 2 tons of refrigeration at two temperature levels (-20 ℃, -70 ℃) was chosen as the design parameters of the problem. A variety of cascade cycle architectures and working fluids were examined to determine the optimum refrigeration system. Their

configurations were different in terms of the type of economization, the cycle to be modified, and the location of the second evaporator. Steady-state thermodynamic modeling was described and established, and the ambient temperatures were the input. The study found that R290/R170 pair is recommended for ULT applications if the flammability risk is eliminated. The suggested system operates at two distinct modes, each with unique cycle architecture. This way, we were able to accomplish a COP increase of 92.3% compared to a conventional two-temperature cascade system with R404A/R508B as their working fluids. The key components' irreversibilities were identified using exergy analysis. Future work is to perform a detailed design based on compressor maps and more advanced heat exchanger models as well as investigate the cycle's performance in other cascade applications.

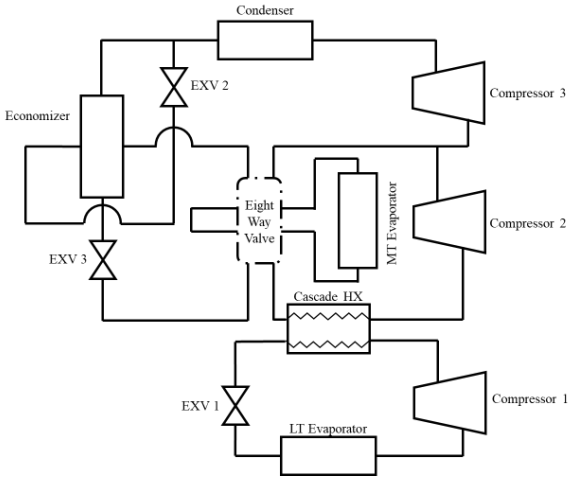

Figure 5: The suggested system schematic diagram

NOMENCLATURE

COP	Coefficient of performance	(–)	s	Specific entropy	$(kJ/kg-K)$
$\dot{E}x_{dest}$	Exergy destruction,	(kW)	$\dot{S}_{gen}$	Entropy generation rate	(kW/K)
g	Gravitational acceleration	(m/s^2)	T	Temperature	$(°C, K)$
h	Specific enthalpy	(kJ/kg)	V	Flow velocity	(m/s)
$\dot{m}$	Mass flow rate	(kg/s)	$\dot{W}$	Power	(kW)
P	Pressure,	(kPa)	z	Elevation	(m)
$\dot{Q}$	Heat transfer rate	(kW)			

Greek symbols

β	Heat source ratio	(–)
ϵ	Second law efficiency	(–)
η_{is}	Isentropic efficacy	(–)

Subscript

amb	Ambient temperature
C	Carnot cycle, theoretical maximum

Acronyms

HFC	Hydrofluorocarbon
LT	Low temperature cycle
MT	Medium temperature cycle

REFERENCES

Abas, N., Kalair, A. R., Khan, N., Haider, A., Saleem, Z., & Saleem, M. S. (2018). Natural and synthetic refrigerants, global warming: A review. *Renewable and Sustainable Energy Reviews*, 557-569.

Aprea, C., & Maiorino, A. (2009). Autocascade refrigeration system: Experimental results in achieving ultra low temperature. *International Journal of Energy Research*, 565-575.

Arpagaus, C., Bless, F., Schiffmann, J., & Bertsch, S. S. (2016). Multi-temperature heat pumps: A literature review. *International Journal of Refrigeration*, 437–465.

ASHRAE. (2018). *2018 ASHRAE Handbook—Refrigeration.* Atlanta: American Society of Heating, Refrigeration and Air-Conditioning Engineers.

Babiloni, A. M., Joybari, M. M., Esbrí, J. N., Royo, C. M., Cervera, Á. B., Albuixech, M. A., & Molés, F. (2020). Ultralow-temperature refrigeration systems: Configurations and refrigerants to reduce the environmental impact. *International Journal of Refrigeration*, 147–158.

Bahman, A. M., Parikhani, T., & Ziviani, D. (2022). Multi-objective optimization of a cold-climate two-stage economized heat pump for residential heating applications. *Journal of Building Engineering*.

Bertsch, S. S., & Groll, E. A. (2008). Two-stage air-source heat pump for residential heating and cooling applications in northern U.S. climates. *International Journal of Refrigeration*, 1282-1292.

Boahen, S., & Choi, J. (2017). Research trend of cascade heat pumps. *Science China Technological Sciences*, pages1597–1615.

Brehm, J. K., Pergantis, E. N., Bani Issa, A. A., Groll, E. A., & Ziviani, D. (2022). Thermodynamic Consideration of Air-Cycles for Ultra-Low-Temperature Applications. *19th International Refrigeration and Air Conditioning Conference at Purdue.* West Lafayette: Purdue e-Pubs.

CDC. (2021, September 29). *Vaccine Storage and Handling Toolkit.* Retrieved from Centers for Disease Control and Prevention: https://www.cdc.gov/vaccines/hcp/admin/storage/toolkit/index.html

Chawla, A. (2020, DECEMBER 11). *Blockchain, IoT to Streamline Global COVID-19 Vaccine Distribution*. Retrieved from Counterpoint Research: https://www.counterpointresearch.com/blockchain-iot-to-streamline-global-covid-19-vaccine-distribution/

Eini, S., Shahhosseini, H., Delgarm, N., Lee, M., & Bahadori, A. (2016). Multi-objective optimization of a cascade refrigeration system: Exergetic, economic, environmental, and inherent safety analysis. *Applied Thermal Engineering*, 804-817.

European Laws Database. (2014, May 20). *Regulation (EU) No 517/2014 of the European Parliament and of the Council of 16 April 2014 on fluorinated greenhouse gases and repealing Regulation (EC) No 842/2006.* Retrieved from EUR-Lex: https://eur-lex.europa.eu/legal-content/EN/TXT/?uri=celex%3A32014R0517

Hwang, Y., Greenfield, B., Kranz, B., Hoaglan, B., Repice, C., Vaisman, I., . . . Elbel, S. (2022, February). Transporting and Storing COVID-19 Vaccines. *ASHRAE Journal*, pp. 12-23.

Klein, S., & Alvarado, F. (2002). Engineering equation solver. *F-Chart Software, Madison, WI*.

Liu, X.-f., Liu, J.-h., Zhao, H.-l., Zhang, Q.-y., & Ma, J.-l. (2012). Experimental study on a −60 °C cascade refrigerator with dual running mode. *Journal of Zhejiang University-SCIENCE A*, 375-381.

Mohammadi, K., & Powell, K. M. (2021). Thermoeconomic Evaluation and Optimization of Using Different Environmentally Friendly Refrigerant Pairs for a Dual-Evaporator Cascade Refrigeration System. *Processes*.

Mouneer, T. A., Elshaer, A. M., & Aly, M. H. (2021). Novel Cascade Refrigeration Cycle for Cold Supply Chain of COVID-19 Vaccines at Ultra-Low Temperature −80˚C Using Ethane (R170) Based Hydrocarbon Pair. *World Journal of Engineering and Technology*, 309-336.

Pfizer. (2022). *COVID-19 Vaccine U.S. Distribution Fact Sheet*. Retrieved from Pfizer: https://www.pfizer.com/news/articles/covid_19_vaccine_u_s_distribution_fact_sheet

Rodríguez-Jara, E. A., Sanchez-de-la-Flor, F. J., Exposito-Carrillo, J. A., & Salmeron-Lissen, J. M. (2022). Thermodynamic analysis of auto-cascade refrigeration cycles, with and without ejector, for ultra low temperature freezing using a mixture of refrigerants R600a and R1150. *Applied Thermal Engineering*.

Sarkar, J., & Agrawal, N. (2010). Performance optimization of transcritical CO2 cycle with parallel compression economization. *International Journal of Thermal Sciences*, 838-843.

Sarkar, J., Bhattacharyya, S., & Lal, A. (2013). Selection of suitable natural refrigerants pairs for cascade refrigeration system. *The Proceedings of the Institution of Mechanical Engineers, Part A: Journal of Power and Energy*, 612-622.

Stegmann, R. (2000, January). Low Temperature Refrigeration. *ASHRAE Journal*, pp. 41-49.

Stoecker, W. F. (1998). *Industrial Refrigeration Handbook.* McGraw-Hill Education.

Sun, J., Li, W., & Cui, B. (2020). Energy and exergy analyses of R513a as a R134a drop-in replacement in a vapor compression refrigeration system. *International Journal of Refrigeration*, 348-356.

Sun, Z., Wang, Q., Xie, Z., Liu, S., Su, D., & Cui, Q. (2019). Energy and exergy analysis of low GWP refrigerants in cascade refrigeration system. *Energy*, 1170-1180.

WHO. (2022). *WHO Coronavirus (COVID-19) Dashboard*. Retrieved from World Health Organization: https://covid19.who.int/